Research Article

In situ stress characteristics of the NE Sichuan basin based on acoustic emission test and imaging logging

Xinxin Fang[1,2] · Hong Feng[2]

© The Author(s) 2021   OPEN

Abstract

This study presents the distribution rule of in situ stress in the northeast Sichuan basin and its relationship with fracture. Sixty-seven sets of core samples of 21 Wells from the terrigenous clastic rock formation (Shaximiao, Qianfoya, Xujiahe) and marine carbonate formation (Jialingjiang, Leikoupo, Feixianguan) in the northeast Sichuan basin were tested by acoustic emission experiment. The in situ stress variation with the depth was established and the corresponding regression analysis was done. The horizontal principal stress direction of terrigenous clastic rock formation and marine carbonate rock formation was obtained by combining the dual diameter data of 6 wells and the imaging logging data of 3 wells. The results show that the vertical stress in the northeast of Sichuan basin has a linear relationship with the depth, and there is little difference between the vertical stress and the overburden weight of rocks. The maximum and minimum horizontal principal stress and horizontal shear stress increase with the burial depth. The divergence degree of horizontal shear stress with depth greater than 3000 m is greater than that of the stratum smaller than 3000 m. The horizontal stress plays a dominant role in the northeast Sichuan basin. With the increase in depth, the influence of tectonic stress field decreases and the vertical stress increases. Impacted by Dabashan and Qinling plate tectonic movement, the direction of in situ stress in marine carbonate strata is nearly east–west. The direction of maximum horizontal principal stress in terrigenous clastic rock formation is basically northwest–southeast. The imaging logging data show that the fracture direction is consistent with the horizontal principal stress direction, and the present in situ stress direction is favorable to the secondary reconstruction of natural fractures, and the fractures keep good opening. The distribution law of in situ stress in northeast Sichuan basin shows $\sigma_H > \sigma_V > \sigma_h$, indicating that the fault activity in this area is dominated by strike-slip type, the tectonic stress field is dominated by horizontal tectonic stress, in addition that the stress state is conducive to reverse fault activity.

Keywords in situ stress · Distribution law · Maximum horizontal principal stress · Minimum horizontal principal stress · Vertical principal stress

1 Introduction

in situ stress is formed under the action of geological tectonic movement and rock mass gravity. After the formation of in situ stress, it changes under the influence of local factors, making its distribution complicated. Practice shows that in situ stress plays an important role in oil and gas exploration and production, drilling operation and borehole wall stability [1–3]. The geological study shows that the northeast Sichuan basin experienced intense compressional orogeny, which forms the present high-steep tectonic belt. This area is characterized as intense

✉ Xinxin Fang, fx15827573109@163.com | ¹China Coal Research Institute, Beijing 100013, China. ²China Coal Technology & Engineering Group Xi'an Institute, Xi'an 710077, Shaanxi, China.

fold and fault, complicated geological situation, strong in situ stress, with broken stratum rock, and the hard and soft interlace, large stratum dip angle, strong stratum anisotropy [4–7]. Due to its complex structural conditions, it is difficult to know the magnitude, direction and transverse distribution of the in situ stress, which leads to many complicated downhole accidents in the process of drilling. The in situ stress is also an extremely important parameter in fracturing operations, which determines the whole fracturing process. For the natural gas reservoirs with carbonate rock and tight sandstone as reservoirs, due to the small porosity and narrow throat, most of them need to be fractured for efficient exploitation. Therefore, it is extremely necessary to study the distribution law of ground stress in northeast Sichuan [8–10].

Scholars at home and abroad have done a lot of research on earth stress in the world. Brady and Brown found that topography, structure and erosion affected in situ stress state [11]. Brown established a quantitative relationship model between in situ stress and depth based on deep measurement data [12]. Hudson believed that the high-level stress was caused by erosion, tectonism, rock anisotropy and other factors [13]. Fuchs K constructed shallow stress distribution characteristics worldwide based on shallow borehole data [14]. Jing F et al. (2008) proposed that geological origin is an important factor for the difference of in situ stress distribution, by studying the distribution characteristics of in situ stress in China's shallow crust [15]. Kang HP et al. (2010) studied the distribution rules of in situ stress in coal mines with different tectonic backgrounds in China and found that tectonic types have an impact on both the magnitude and direction of in situ stress [16].

Presently, most of the methods used by Chinese scholars to study the distribution of in situ stress refer to Brown&Hoek (1978). These two scholars conduct deep research on the in situ stress worldwide, which has certain reference significance for engineering construction and shallow mineral resources development. According to the ideas of Brown&Hoek, Chinese scholars Zhao DA, Jing Fe, Zhu HC, Kang HP and others have studied the distribution law of in situ stress in shallow strata of China and established the in situ stress database [17–19]. The results show that the ratio of horizontal stress to vertical stress measured in China is larger than the stress level of Brown–Hoek envelope, and the maximum stress envelope is basically consistent with the Brown–Hoek envelope, while the minimum stress envelope is smaller than the Brown–Hoek envelope. Although these scholars have made some achievements in their research on the distribution law of in situ stress in China, they are mainly applicable to the shallow crust with a burial depth of less than 300 m, but not to the deep strata of Sichuan Basin. There is no systematic research on the distribution law of ground stress in the northeastern of Sichuan Basin at present.

In this paper, more than 67 in situ stress data are selected from P and Y gas fields in the northeast Sichuan basin, mainly from acoustic emission test method. Scatter plots of vertical and horizontal in situ stress with depth in the northeast Sichuan basin are established, and the variation characteristics of horizontal shear stress and lateral pressure coefficient with buried depth are studied, as well as the in situ stress orientation of continental and marine strata in the northeast Sichuan basin.

2 Geological setting

Sichuan Basin belongs to the Sichuan platform depression of Yangzi platform. After the consolidation of the basement after the Jinning movement and Chengjiang movement, the platform began to develop steadily. In the northwestern of Sichuan Basin, Longmen Mountain platform margin fault-fold belt is transformed into Songpan-Ganzi geosyncline fold system [20–23]. The northeast side is the Daba Mountain platform margin fault-fold belt, the transition to the Qinling geosyncline fold system. The southeast and southwest sides are Yunnan, Guizhou, Sichuan, Hubei platform fold belt. The basin is lozenge shaped and distributed roughly in NE direction, which reflects that the evolution of the deep lozenge-shaped faults in the Yangtze platform controls the formation of the Sichuan basin and the generation, development and distribution of folds within the basin. The sedimentary evolution of the whole Sichuan basin includes platform sedimentary stage dominated by marine carbonate rocks and basin sedimentary stage dominated by terrestrial clastic rocks. The lithology of marine carbonate rocks is limestone, dolomite and paste rock, while that of terrigenous clastic rocks is sand and mudstone (Fig. 1). Northeast Sichuan lies in the front of Daba Mountain and the northern end of eastern Sichuan high-steep structural belt, which belongs to the intersection area of the arc thrust structural belt of Southern Daba Mountain and the NE fold belt of eastern Sichuan. The basement in northeast Sichuan basin was formed during the Jinning Movement, which ended the geological development history of pre-Sinian, and entered the stage of platform development in Sinian-Triassic. During the development and evolution of the Tethys tectonic domain and the coastal pacific tectonic domain from the Indosinian to the Himalayan period, the northeast Sichuan structure was formed through multiple periods of superposition and transformation under the action of long-term compressive strength alternation in the Upper Yangtze region, and finally located in the late Himalayan period [24–28].
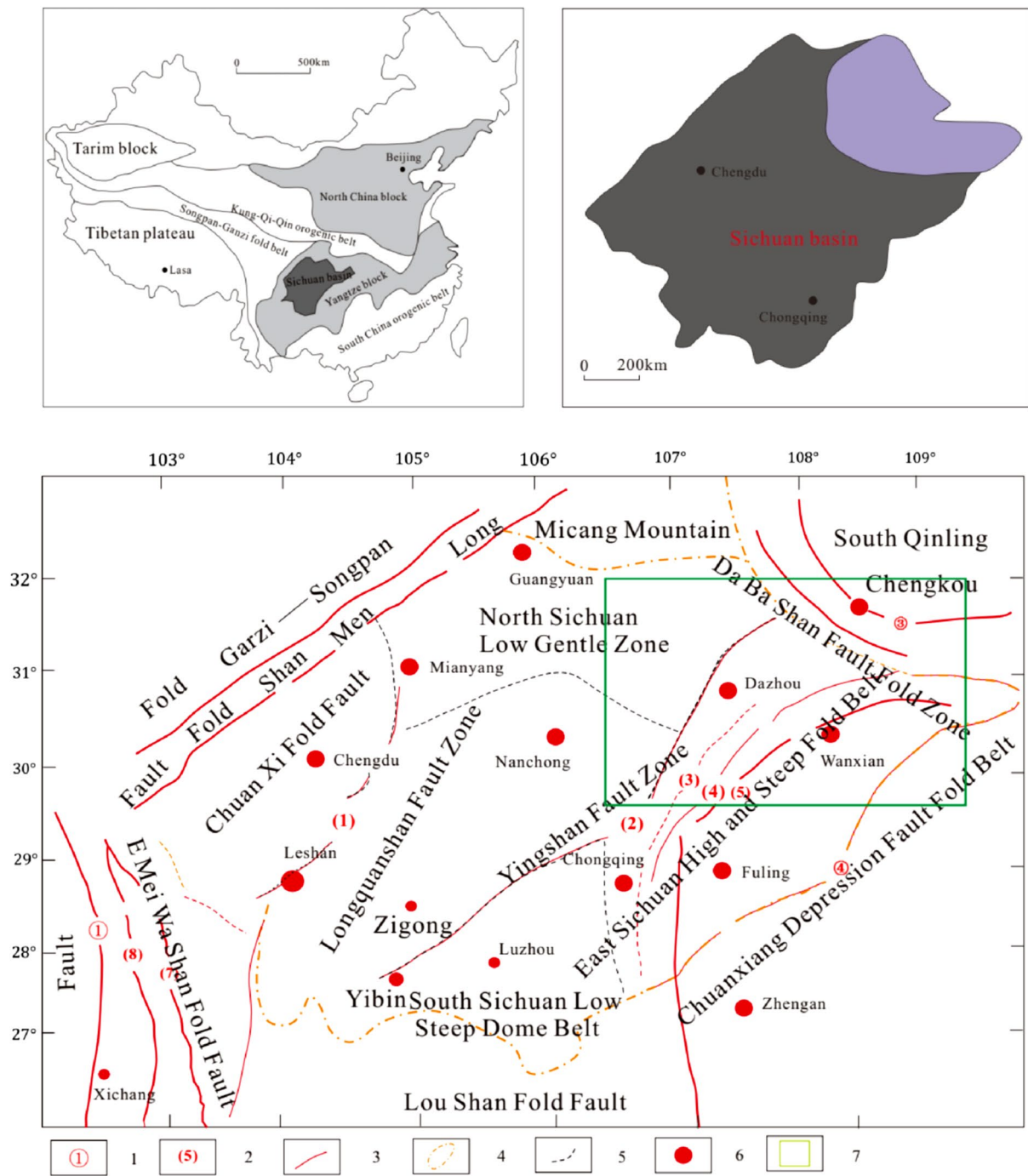
1.Deep and large lithospheric faults: ①Anning River, ②Longmen Mountain, ③Chengkou, ④ Qiyao Mountain;2. Deep and large crustal faults: (1) Peng Guan, (2) Xiongpo, (3) Long Quan Mountain, (4) Huaying Mountain, (5) Wuxi-Tiexi, (6) Huangnitang, (7) Emei-Washan, (8) Ganluo-Xiaojiang;3. Large deep faults in the caprock (including basement faults);4. Basin scope;5. Techtonic unit;6. City;7. Studied area.

Fig. 1 Regional structural map of Sichuan Basin

The Indosinian tectonic stress field in the northeast Sichuan basin is controlled by the orogenic belt at the margin of the basin, presenting a state of compressional stress around the basin [29, 30]. In the northwestern of Longmen Mountain area, due to the closure of Songpan-Ganzi trough, caused the thrusting nappe of the Longmenshan from northwest to southeast, the direction of stress field is NW–SE, and the main compressive stress direction is from NW to SE extrusion. On the north side of Micang Mountain, due to the subduction and closure of Mianlue small ocean basin in Qinling Mountains, Mianlue suture zone was formed, and Qinling fold uplifted, resulting in compression stress field from north to south, and compression of principal stress direction from north to south. On the northeast side of Daba Mountain, the subduction and collision of Qinling plate and Yangtze Plate caused the folding and uplift of Daba Mountain and thrust nappe, forming the NW direction of folding and thrust belt. The direction of stress field is NE-SW direction, and the main compressive stress is extrusion from NE-SW. The southeast Sichuan basin is mainly affected by the uplift of Xuefeng Mountain orogenic belt, which produced a NE-NW stress field, and the main compressive stress was mainly squeezed from SE to NW (Figs. 2, 3).

3 Methods

3.1 Acoustic emission method

3.1.1 Rock samples

Terrigenous clastic rocks and marine carbonate reservoirs are mainly developed in the northeastern of Sichuan basin. The experimental rock samples are the sandstone and carbonate cores from wells, i.e., P-101, P-114, P-136 of P gas field and Y-210, Y-107 of Y gas field, in the northeastern of Sichuan basin. The sandstones are from Shaximiao Formation, Qianfoya Formation and Xujiahe Formation, and the carbonate rocks are from Leikoupo Formation, Jialingjiang Formation and Feixianguan Formation. In order to avoid core damage under low load during preloading, the integrity of the core is guaranteed. According to the rock mechanics sample standard, the full-size core is machined into a standard cylindrical shape of ϕ25 mm and length 50 mm (Fig. 4). The parallelism of both ends of the sample meets the requirements to avoid excessive noise in the process.

In the experiment, it is assumed that the rock formation is approximately horizontal before it is subjected to the maximum stress. A rectangular coordinate system is established according to the right-hand rule, where X and Y correspond to the strike and inclination of the rock formation, and Z is upward along the orthogonal plane. The sample is drilled from six directions: X, X45°Y, Y, Y45°Z, Z45°X and Z. The test piece was processed into a cylinder with a diameter of 25 mm and a length of 50 to 80 mm, and the end treatment is performed. Perform a uniaxial compression test on the loader, as well as observe and record the acoustic emission activity during this process.

3.1.2 Experimental device

The experimental instrument is composed of MTS816 rock testing system (Fig. 5) and SAMOS™ acoustic emission detection system (Fig. 6). MTS816 rock test system is an all-digital computer automatic control system, which can record load, stress, displacement and strain values in real time and draw load–displacement, stress–strain curves synchronously. SAMOS™ acoustic emission detection system is the third generation of digital system developed by PAC. Its core is PCI-8 acoustic emission function card which processes PCI bus in parallel, and it has the capability of real-time acoustic emission feature extraction, waveform collection and processing with 8 channels on one board. It adopts modern digital signal processing technology (DSP) and is the most advanced acoustic emission processing system in the world.

3.1.3 Determination of Kaiser effect point

Boyce conducted tests on the whole acoustic emission process of various rocks and established a general mode of the acoustic emission process of brittle rocks (Fig. 7). In section AB, the initial crack of the sample gradually closed, accompanied by more acoustic emission signals, but usually messy. However, in the DF section, acoustic emission activities increase sharply, and rock samples are in a state of instability. Therefore, the characteristic points of Kaiser effect exist in the BC-CD stage.

3.1.4 Processing method of experimental data

Due to the discreteness of AE, anisotropy of mechanical properties of rock and measurement error, the measured results of different specimens in the same direction are different to some extent, so statistical analysis must be made. According to whether the Kaiser effect is obvious or not, certain weights are given, respectively, and then weighted average [31]. For those with obvious Kaiser effect, the weight P equals 1. For the insignificant ones, P is given 0.5. Lastly, P is given 0, for those not obvious or not been determined at all. Then, the optimal value σ_0 for each orientation is obtained:
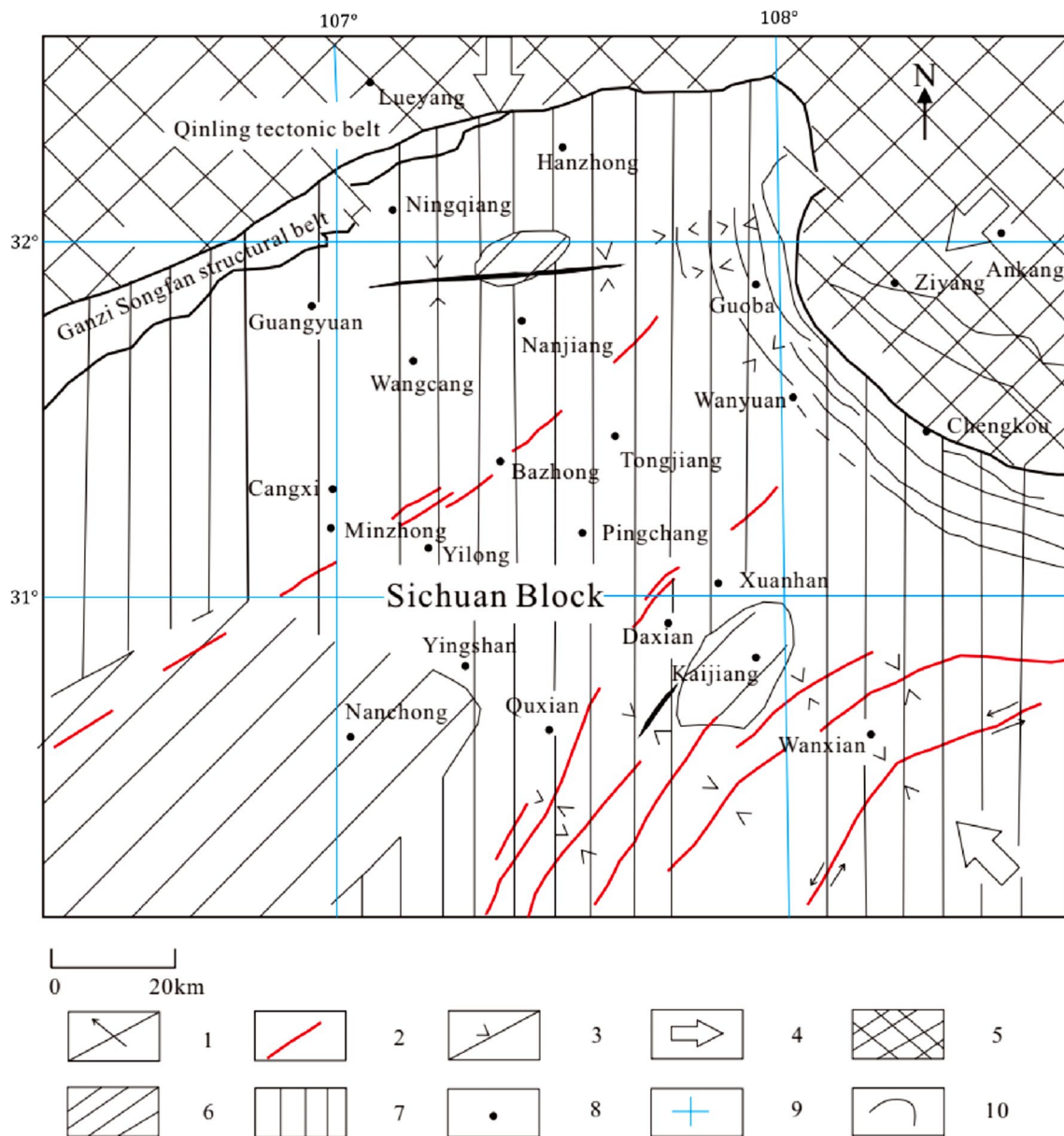
1-Fault (Arrows indicate the tendency of fault plane).2-Basement fault.3-Local tectonic stress field.4-Regional stress field.5-Uplift.6-Relative uplift.7-Depression basin.8-City.9-Latitude and longitude.10-Tectonic zoning zone

Fig. 2 Paleo-tectonic and paleo-tectonic stress field in northeast Sichuan

$$\sigma_0 = \sum_{i=1}^{n} P_i \sigma_i / \sum_{i=1}^{n} P_i \quad (1)$$
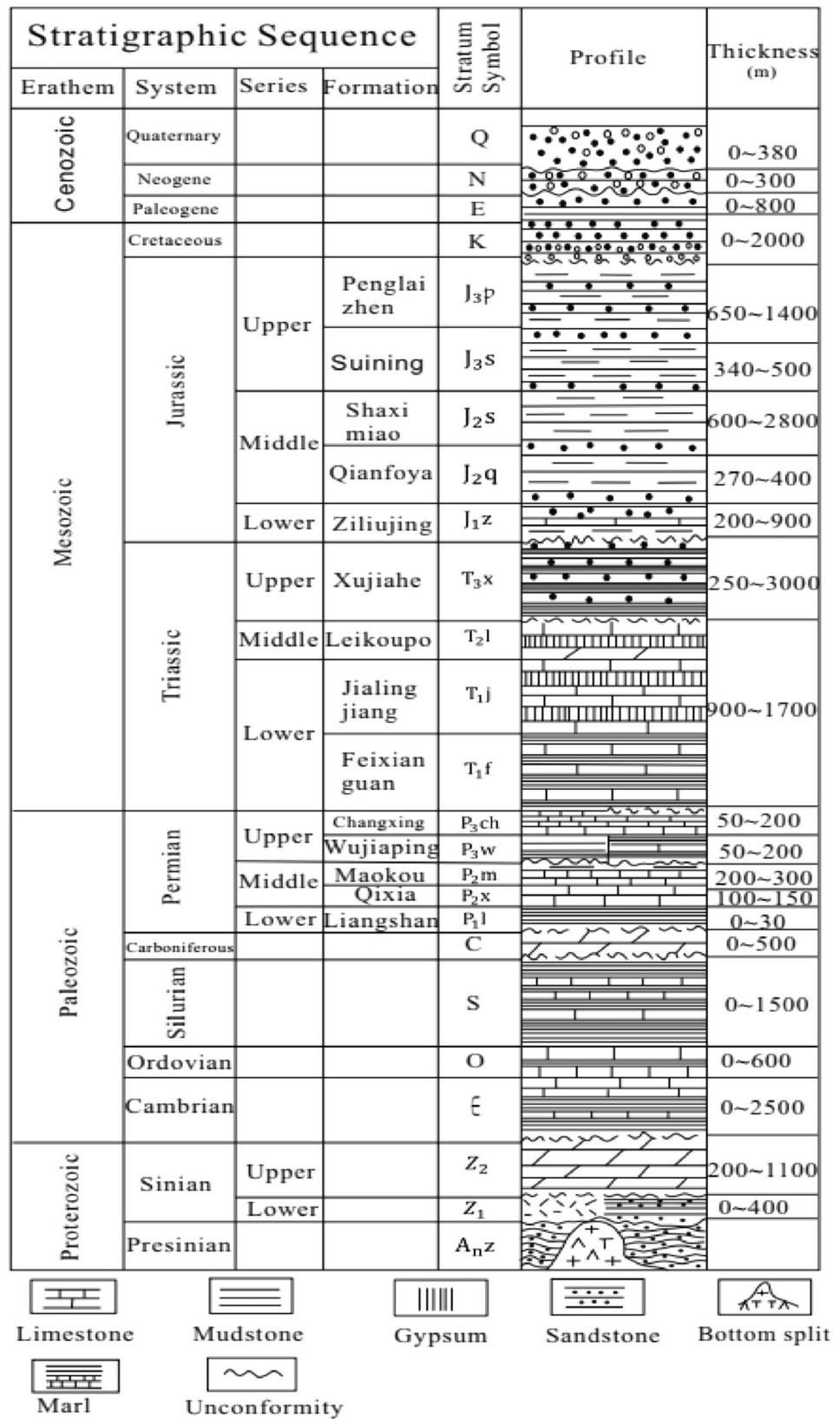
where n is the number of specimens at a certain orientation, σ_i ($i = 1,2,3 \ldots n$) is the measured value of specimens, and P_i is the weight of test results.

According to the calculation formula of the horizontal plane stress state:

$$\sigma_1 = \frac{\sigma_x + \sigma_y}{2} + \frac{|\sigma_x - \sigma_y|}{2} \sqrt{1 + \tan^2 2\alpha} \quad (2)$$

$$\sigma_2 = \frac{\sigma_x + \sigma_y}{2} - \frac{|\sigma_x - \sigma_y|}{2} \sqrt{1 + \tan^2 2\alpha} \quad (3)$$

Fig. 3 Comprehensive histogram of Sichuan basin strata. (Adapted from Yang Zhibin [13])
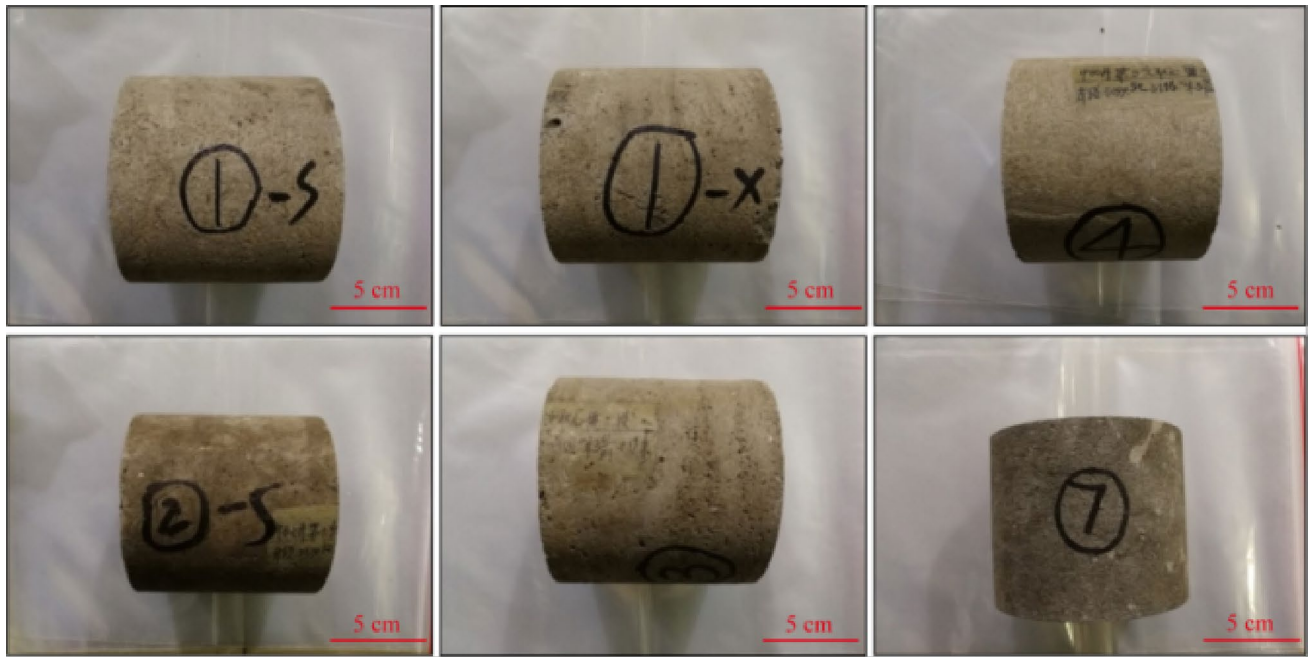

Stratigraphic Sequence				Stratum Symbol	Profile	Thickness (m)
Erathem	System	Series	Formation			
Cenozoic	Quaternary			Q		0~380
	Neogene			N		0~300
	Paleogene			E		0~800
Mesozoic	Cretaceous			K		0~2000
	Jurassic	Upper	Penglai zhen	J_3p		650~1400
			Suining	J_3s		340~500
		Middle	Shaximiao	J_2s		600~2800
			Qianfoya	J_2q		270~400
		Lower	Ziliujing	J_1z		200~900
	Triassic	Upper	Xujiahe	T_3x		250~3000
		Middle	Leikoupo	T_2l		
		Lower	Jialingjiang	T_1j		900~1700
			Feixianguan	T_1f		
Paleozoic	Permian	Upper	Changxing	P_3ch		50~200
			Wujiaping	P_3w		50~200
		Middle	Maokou	P_2m		200~300
			Qixia	P_2x		100~150
		Lower	Liangshan	P_1l		0~30
	Carboniferous			C		0~500
	Silurian			S		0~1500
	Ordovian			O		0~600
	Cambrian			E		0~2500
Proterozoic	Sinian	Upper		Z_2		200~1100
		Lower		Z_1		0~400
	Presinian			A_nz		

Limestone   Mudstone   Gypsum   Sandstone   Bottom split

Marl   Unconformity

Fig. 4 Full diameter core samples of part carbonate rocks

Fig. 5 Rock testing system


Fig. 6 Acoustic emission detection system

When the principal stress is changed counterclockwise to σ_x, the direction is positive, and negative versa.

3.2 Determination of in situ stress direction

It is still one of the most effective methods to determine the direction of in situ stress based on the borehole wall break-out method. The stress avalanche of the borehole wall rock is a form of shear fracture [32, 33], which meets the Mohr–Coulomb condition:

$$\tau \geq c_0 + \sigma_V \cdot \tan \varphi \tag{5}$$

$$\tan 2\alpha = \frac{\sigma_x + \sigma_y - 2\sigma_{xy}}{\sigma_x - \sigma_y} \tag{4}$$

where σ_x, σ_y and σ_{xy} are the experimental acoustic emission values in the directions of 0°,45° and 90°, respectively, MPa; σ_1 is acoustic emission interpretation of the maximum horizontal principal stress, MPa; σ_2 is acoustic emission interpretation of minimum horizontal principal stress, MPa; α is azimuth of maximum horizontal principal stress.

Fig. 7 General acoustic emission mode in the process of rock fracture
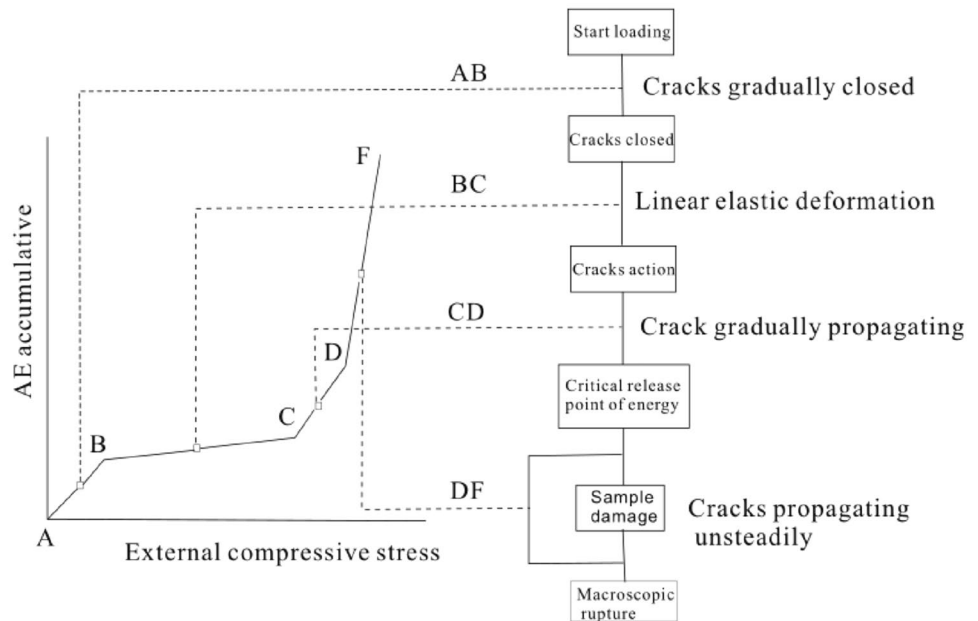
where τ is the shear fracture stress of the rock, MPa, which is composed of two parts. One is the cohesion c_0; the other is internal friction force, equal to the product of the normal stress of the failure surface and the internal friction coefficient (φ, the internal friction angle of the rock; the tangent value of φ is the internal friction coefficient of the rock).

When stress caving occurs during drilling, the long axis direction of the ellipse is parallel to the minimum horizontal principal stress direction. In order to accurately determine the location of the borehole producing stress caving and the long axis direction of the elliptical borehole, the hole wall must meet the width of the caving section greater than 6 cm (larger than the width of the tool plate). The caving section must have sufficient length, generally at least 30 cm (larger than the length of the tool plate). The caving section has to be deep enough that the difference between the two logging curves is greater than 1 in (1 in. = 25.4 mm). The difference between the short-axis diameter curve and the bit diameter curve is limited to 0.5 in, and the deviation is less than 5°. In the actual data processing, the dual well diameter curves $C_{1,3}$, $C_{2,4}$, the relative azimuth curves R_B and deviation azimuth curve A are used to determine the long axis orientation of the elliptical borehole (stress caving borehole orientation). Azimuth A and plate azimuth R_B (referring to the clockwise angle between plate 1 azimuth and well inclination azimuth) were recorded during dip logging, and then, the direction of the minimum horizontal principal stress (α) is:

$$\alpha = A + R_B, \quad C_{1,3} > C_{2,4} \tag{6}$$

$$\alpha = A + R_B + 90°, \quad C_{1,3} \leq C_{2,4} \tag{7}$$

In addition, the orientation of in situ stress can be determined from the characteristics of borehole wall caving, pressure fractures, stress release fractures and shear wave anisotropy on full borehole formation microresistivity scanning imaging (FMI) and downhole acoustic television imaging logging (BHTV, CBIL).

4 Results

The variation characteristics of the in situ stress value with depth reflect the stress state of the shallow part of the crust to some certain extent. The analysis of the crustal stress characteristics through in situ stress measurement data has always been a problem explored by geoscientists. In order to show the distribution law of in situ stress reflected by measured points directly, the stress values of 67 core samples in the study area were analyzed by using the measured data and the method of linear regression analysis, achieving the relations of vertical principal stress, maximum horizontal principal stress and minimum horizontal principal stress with depth. The horizontal principal stress direction of terrigenous clastic rock and marine carbonate rock formation is obtained from imaging logging data. The in situ stress value obtained by acoustic emission is compared with that calculated by logging method to verify the reliability of logging method.

4.1 Variation law of vertical stress with burial depth

A statistical analysis of vertical stress σ_V in the northeastern of Sichuan is made on the basis of acoustic emission experimental data. As the in situ stress in shallow strata is greatly affected by topography, the data with burial depth less than 100 m are not considered in this statistical analysis. The variation of vertical in situ stress in Northeast Sichuan Basin with burial depth is shown in Fig. 8. Figure 8 shows that although the vertical in situ stress in the northeastern of Sichuan Basin has a certain degree of dispersion, generally, it increases continuously with the increase in buried depth and changes in a linear relationship, similar to the statistical results of Hoek&Brown as well as Zhu Huanchun.
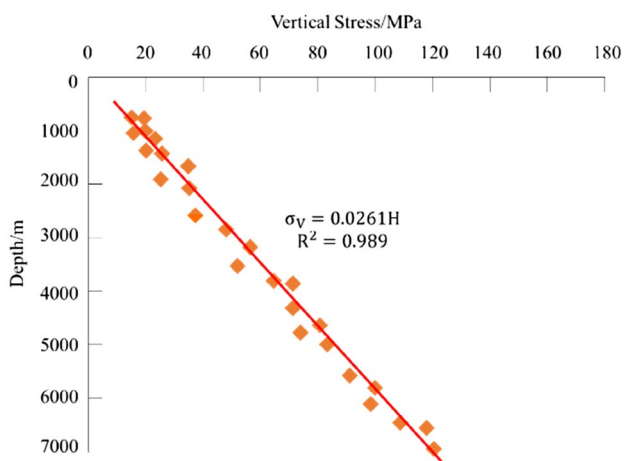
Fig. 8 The variation of vertical in situ stress with buried depth

After linear regression, the regression formula of vertical stress in the northeastern part of Sichuan basin with burial depth can be obtained as follows:

$$\sigma_V = 0.0261H, \quad R^2 = 0.989 \tag{8}$$

where H is the buried depth, m; σ_V is the vertical in situ stress, MPa.

According to the variation of vertical in situ stress with buried depth, the overall bulk density of overlying rock is about 25–30 kN/m^3. Therefore, the variation of vertical stress with buried depth in Northeast Sichuan is approximately similar to the rock bulk density. It is further indicated that the main component of vertical in situ stress σ_V is rock dead weight.

4.2 Variation of horizontal principal in situ stress with buried depth

The scatter distribution of the maximum and minimum horizontal principal in situ stress in northeast Sichuan basin with buried depth is shown in Fig. 9, which shows a linear correlation with buried depth on the whole. Linear regression is performed, achieving the regression equation of the maximum and minimum horizontal principal in situ stress with the buried depth, as shown in Table 1.

It can be seen from Fig. 9 that although the maximum and minimum horizontal principal in situ stress in northeast Sichuan basin has certain discreteness, they generally show an increasing trend with the increase in depth. It can be seen from Table 1 that the regression equation consists of coefficient term and product ones. The coefficient term
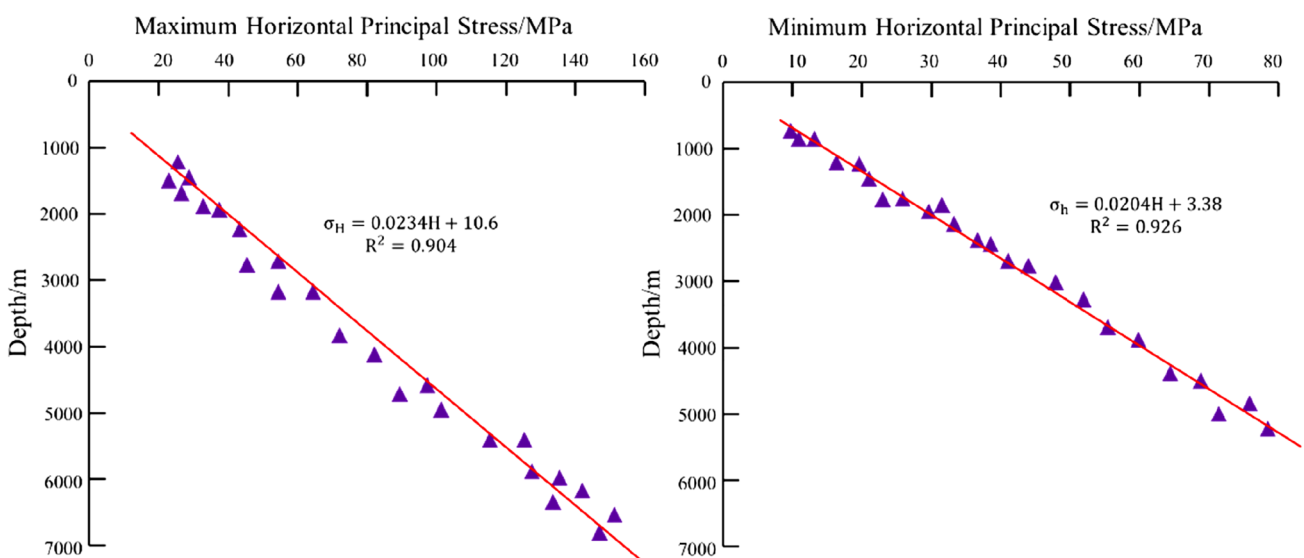

Fig. 9 Variation of horizontal principal in situ stress with buried depth in Northeastern Sichuan

Table 1 Regression coefficients of horizontal principal in situ stress in the northeastern of Sichuan

Area	Stress type	Coefficient	Constant	R^2
Northeastern Sichuan	σ_H	0.0234	10.6	0.904
	σ_h	0.0216	3.16	0.931

Table 2 Regression coefficients of horizontal principal stresses in other basins in China (Ge Hongkui, 1998)

Area	Stress type	Coefficient	Constant
North China Plain	σ_H	0.03	−10.5
	σ_h	0.021	−5.87
Qaidam Basin	σ_H	0.03	−22.58
	σ_h	0.022	−11.65
Songliao Basin	σ_H	0.0266	−2.34
	σ_h	0.0182	−0.777
Bohai Bay Basin	σ_H	0.022	0.7
	σ_h	0.018	0.5
Western Sichuan	σ_H	0.0207	3.38
	σ_h	0.0192	1.16

represents the variation degree of horizontal principal in situ stress and the constant term represents the in situ stress in the shallow strata. Compared with the coefficient term of vertical stress, the coefficient term of maximum and minimum horizontal stress is less than the corresponding value of vertical stress, indicating that the variation degree of vertical stress with buried depth is greater than that of horizontal principal stress.

The value of constant term in Northeast Sichuan is larger than that in West Sichuan, indicating that the value of in situ stress in shallow northeast Sichuan is larger than that in the western of Sichuan. Compared with the horizontal in situ stress of other basins in China, the regression coefficient of the maximum horizontal principal stress of Sichuan Basin is less different from that of Bohai Bay basin, but less than that of North China plain, Qaidam basin and Songliao basin (Table 2). It shows that the variation degree of maximum horizontal principal stress with depth in Sichuan basin is smaller than that in other basins. Compared with other basins, the minimum horizontal principal stress of Sichuan Basin has little difference, indicating that the minimum horizontal principal stress of these blocks varies with depth to similar degree. However, the constant term of Sichuan basin is positive, the constant term of Songliao basin, North China plain and Qaidam basin is negative, and the constant term of Bohai Bay basin is positive, but less than that of Sichuan Basin, indicating that a certain amount of horizontal principal stress still exists

in the shallow crust of Sichuan basin. The shallow parts of Songliao basin, North China plain and Qaidam basin are in the state of under pressure equilibrium, while the shallow parts of Bohai Bay basin are in the state of stress equilibrium.

4.3 Variation law of lateral pressure coefficient and horizontal shear stress with buried depth

k is often used to characterize the lateral pressure coefficient, which is often used to describe the stress state at a certain point. A large number of studies have shown that the vertical stress is generally close to the dead weight of rock mass, especially for deep rock mass, indicating that horizontal stress and dead weight of rock mass can be used to represent the stress state at a certain point. Brown–Hoek used $\frac{\sigma_H + \sigma_h}{2\sigma_V}$ to study the distribution law of internal stress in the world. The formula is the ratio between average horizontal principal stress (that is, the mean value of the maximum and minimum horizontal principal stress) and vertical principal stress. In this paper, a similar method is used to analyze the variation of lateral pressure coefficient with depth in the northeast Sichuan basin.

Assuming that the ratio of the average horizontal stress to the vertical stress is k, k is the lateral pressure coefficient:

$$k = \frac{\sigma_H + \sigma_h}{2\sigma_V} \tag{9}$$

Assuming again: $k = \frac{a}{H} + b$, $\frac{1}{H} = x$, a and b are regression coefficients, respectively, and it can be considered that k is in a linear relationship with the reciprocal of depth.

Before regression, the lateral pressure coefficient and $1/H$ are linearized to obtain the regression formula of the lateral pressure coefficient and depth in the northeastern of Sichuan, as shown in Eq. (10), and the inner and outer envelope curves are shown in Fig. 10.

$$k = \frac{181.72}{H} + 0.85 \tag{10}$$

The variation trend of lateral pressure coefficient k in Northeast Sichuan with depth is obtained by referring to the Hoek–Brown method of in situ stress analysis, statistics and fitting (Fig. 10). The variation trend of outermost and innermost envelope is obtained by fitting based on the points on the boundary (Fig. 10), which are used to define the variation range of k in northeast Sichuan and characterize its distribution rule. In the shallow buried depth less than 800 m, the lateral pressure coefficient in
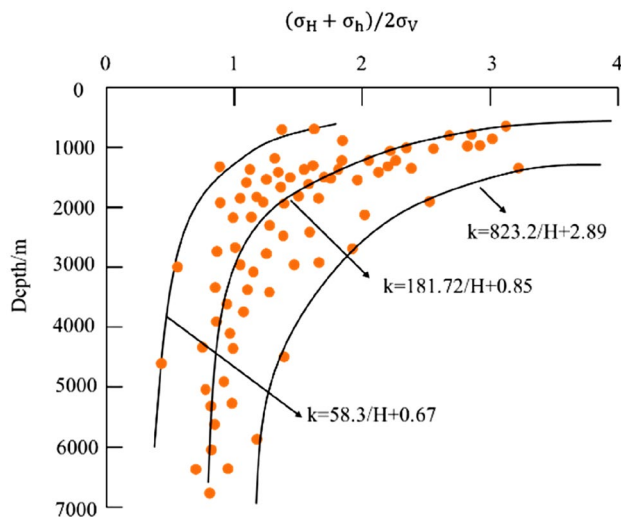
Fig. 10 The ratio of the horizontal average in situ stress to the vertical stress in Northeast Sichuan
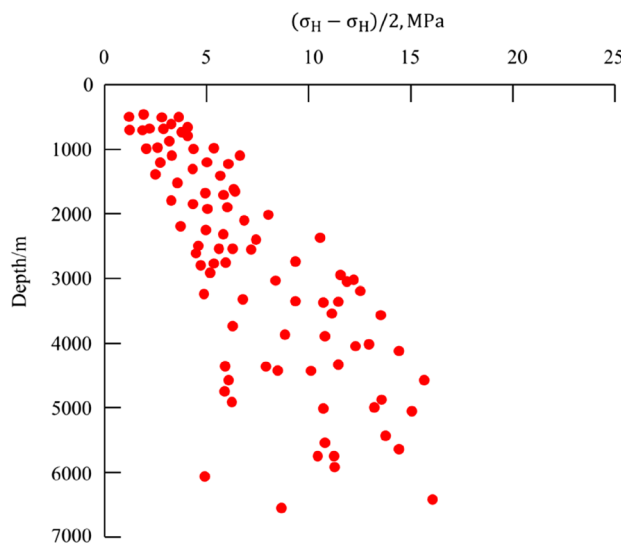

Fig. 11 Distribution of horizontal shear stress with depth in the northeastern of Sichuan

the northeastern of Sichuan varies from 1 to 2. However, when the depth is more than 1000 m, the lateral pressure coefficient in the northeastern of Sichuan basin decreases slowly with the depth, indicating that the horizontal tectonic stress in the northeastern of Sichuan basin is dominant. With the increase in depth, the influence of tectonic stress field decreases and the vertical stress increases.

Tanaka et al. believed that the rupture phenomenon in the crust of earth was very complicated. Macroscopically, it is the sliding failure caused by the increase in shear stress. Therefore, it is of great significance to understand the shear stress of strata for analyzing the conditions of

fault slip. The distribution diagram of horizontal shear stress in the northeastern of Sichuan basin with buried depth (Fig. 11) shows that the horizontal shear stress in the northeastern of Sichuan basin has a linear relationship with buried depth. In the terrigenous clastic rocks (buried depth less than 3000 m), the horizontal shear stress is 0.2–9.8 MPa. In the marine carbonate strata (buried depth greater than 3000 m), the horizontal shear stress is 10–20 MPa, and the dispersion degree is greater than that of terrigenous clastic strata.

4.4 Horizontal principal stress direction

4.4.1 Terrigenous clastic rock formations (depth less than 3000 m)

In terrigenous clastic rock formations, the direction of the horizontal principal stress is determined mainly by determining the direction of the long and short axis of the borehole based on caliper logging data. According to 26 sets of the data of caliper logging data of Y1, Y103 and Y115, a rose diagram of the maximum horizontal principal stress in the longitudinal direction was made (Fig. 12). It can be seen that the direction of the maximum horizontal principal stress in the terrane clastic rock formation (Shaximiao Formation, Qianfoya Formation and Xujiahe Formation) is basically NW–SE direction, i.e., 97.5°–112.5°.

4.4.2 Marine Carbonate Formation (buried depth greater than 3000 m)

4.4.2.1 Determination of the horizontal principal stress direction with drilling-induced fractures The marine carbonate formation has special lithological characteristics. The imaging logging data of the Y115 well in northeastern Sichuan show that the borehole of the marine carbonate formation is in good condition, and the borehole collapse in FMI image is not obvious. The CAL1 and CAL2 double calipers do not calculate the direction of the well wall caving, but from the FMI image, it can be seen that there are obvious drilling-induced fractures, i.e., the cracks formed around the hole wall due to heavy mud fracturing or stress release. Therefore, drilling-induced fractures and stress release fractures are mainly used to analyze the direction of in situ stress in the marine carbonate formations. The analysis of fracturing-induced fractures mainly refers to the fact that vertical fractures can be generated when specific gravity of the drilling fluid is too large during the drilling process. When the formation is drilled open, the stress release fracture may be generated due to the release of the in situ stress. It is an induced fracture produced during the drilling process. The direction of the
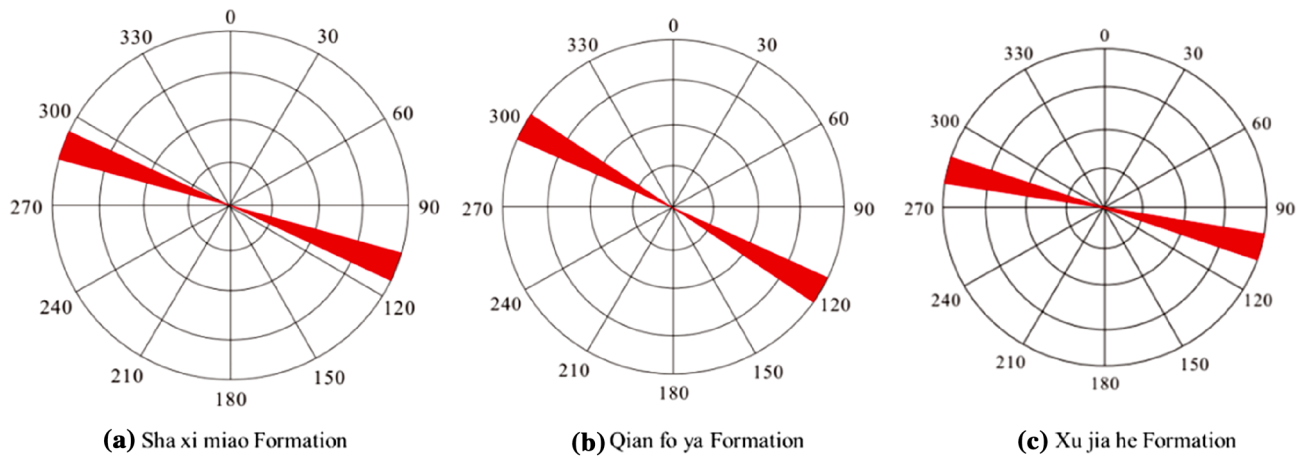
(a) Sha xi miao Formation   **(b)** Qian fo ya Formation   **(c)** Xu jia he Formation

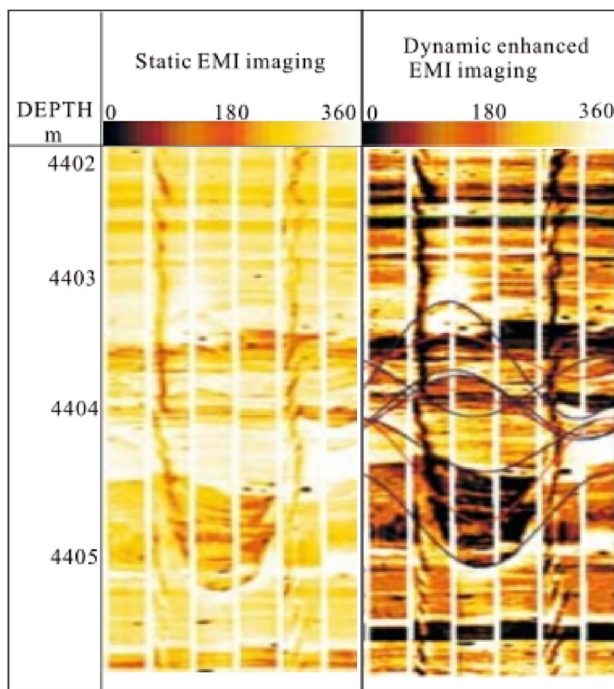**Fig. 12** In situ stress azimuth of terrigenous clastic rock formation

Fig. 13 The NE-SW orientation shown by the drilling-induced fracture with EMI

stress release fracture expresses the direction of the current maximum horizontal principal stress.

In order to analyze the direction characteristics of in situ stress in each longitudinal marine carbonate strata in detail, the direction distribution of maximum horizontal principal stress in marine carbonate strata was obtained by statistical analysis of the direction of induced fractures based 33 sets of data of the studied area (Fig. 13). It can be

seen that the direction of maximum principal stress is in the direction of NE-SW, ranging from 55° to 88.5° (Fig. 14).

4.4.2.2 Determination of horizontal principal stress direction by borehole wall breakout method The borehole wall caving is the shear failure caused by stress concentration near the borehole wall, and the direction of the caving is consistent with the direction of the minimum horizontal principal stress. Taking the P-101 well from P gas field as an example, the EMI data shown in Fig. 15 show the borehole wall caving. The direction of the caving is near southwest–northeast; that is, the direction of the minimum horizontal principal stress is southwest–northeast. Statistics show that its maximum horizontal principal stress direction is NE-SW, ranging from 62°–85° (Fig. 16).

5 Discussion

5.1 The relationship between in situ stress and geological structure

The distribution law of in situ stress in northeastern Sichuan shows $\sigma_H > \sigma_V > \sigma_h$, indicating that the fault activity in this area is dominated by strike-slip type, the tectonic stress field is dominated by horizontal tectonic stress, in addition that the stress state is conducive to reverse fault activity. From the analysis of the tectonic evolution history in northeast Sichuan, it can be seen that the area has been subjected to multi-phase and multi-directional compressive stress from the fold belt of eastern of Sichuan, Daba Mountain and other peripheral mountain systems. Especially during the Yanshan-Xishan tectonic movement, this area and the South Qinling Mountains
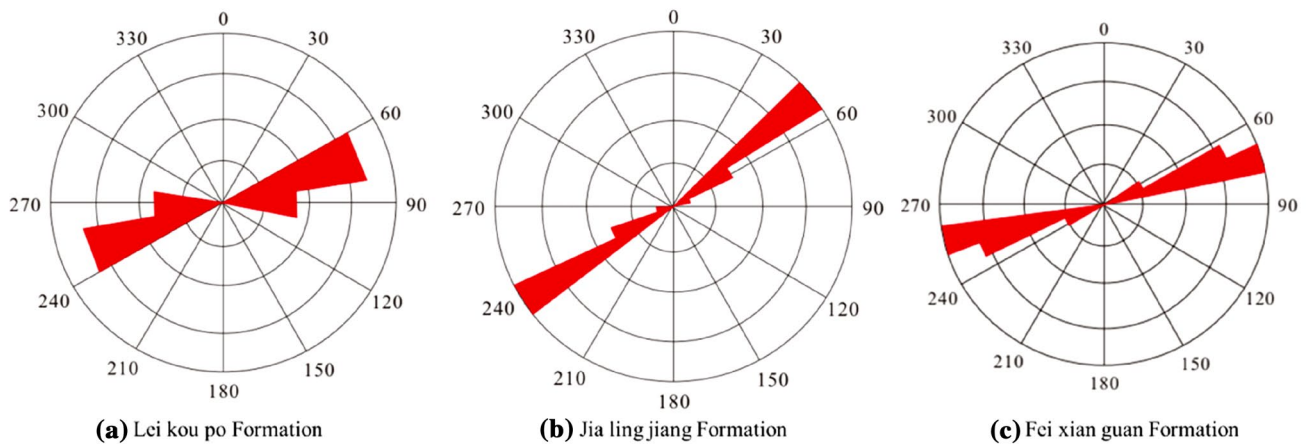
(a) Lei kou po Formation

(b) Jia ling jiang Formation

(c) Fei xian guan Formation

Fig. 14 Direction of horizontal principal stress in marine carbonate formations
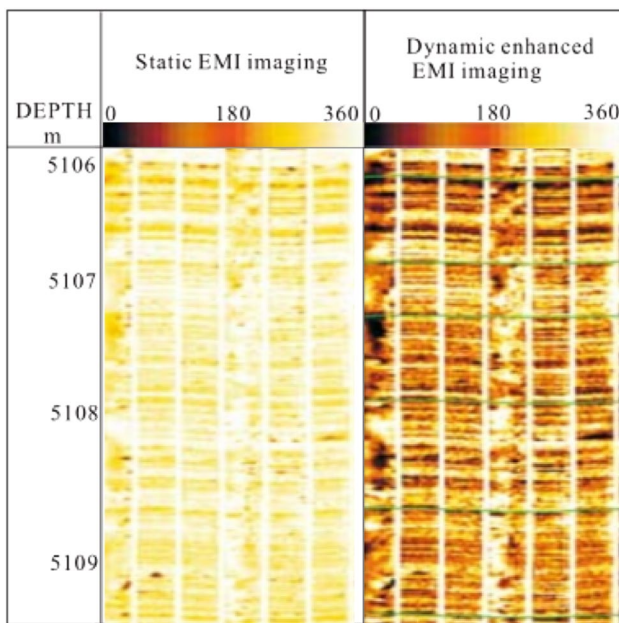
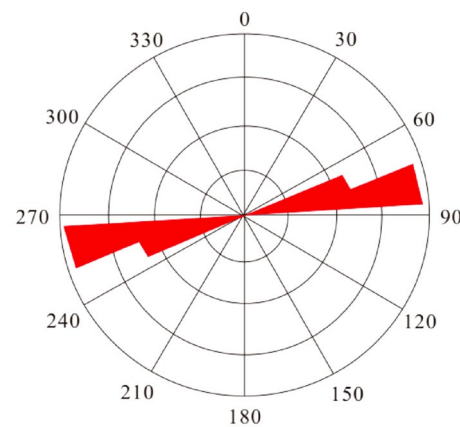**Fig. 15** The SW to NE orientation shown in the borehole caving by EMI in the Feixianguan Formation

Fig. 16 Direction of maximum horizontal principal stress of wall caving azimuth statistics in the Feixianguan Formation

were strongly compressed from north to south, resulting in strong compression folds, thrust nappe and tectonic uplift, leading to the Dabashan trend. The interior of the basin is squeezed and thrusted, and the in situ stress affected the interior of the basin through conduction, and gradually attenuated until it disappeared. From the orogenic belt to the basin, the strength of structural deformation was obviously weakened. For strata with a buried depth of less than 3000 m; that is, terrigenous clastic rock strata, the corresponding shear stress dispersion and its value are less than the buried depth and greater than 3000 (marine carbonate rock formation), which corresponds to the dispersion degree, indicating that the structural

characteristics of marine carbonate rock strata are more complex than terrigenous clastic ones, which is conducive to the accumulation of stress and is easy to induce strong tectonic movement.

The direction of in situ stress of Marine carbonate strata is NE-SW, while the subduction and collision of Daba Mountain, Qinling plate and Yangtze Plate in northeast Sichuan make the Daba Mountain fold uplift and thrust nappe, forming the NW fold and thrust belt, resulting that the direction of stress field formed is also NE-SW. It furthermore shows that the formation of marine carbonate strata in this area is influenced by the geological movement in this period.

5.2 The relationship between fracture and in situ stress direction

Horizontal principal stress is the fundamental driving force for the formation of fractures. When the local stress

direction is consistent with the crack strike, in situ stress has a secondary transformation effect on natural fractures, which is conducive to the maintenance of open state and efficient conductivity of natural fractures. On the contrary, natural fractures will reduce their conductivity when squeezed by in situ stress. It can be seen from Fig. 14 that the fracture direction of marine carbonate strata in Northeast Sichuan basin is in good consistency with the horizontal principal stress direction. The in situ stress direction is favorable to the secondary reconstruction of natural fractures, and the fractures keep good opening.

According to the classification of in situ stress [34], the three basic types (I, II, III) of in situ stress directly determine the occurrence of hydraulic fractures. I: $\sigma_V > \sigma_h > \sigma_H$. II: $\sigma_H > \sigma_h > \sigma_V$. III: $\sigma_H > \sigma_V > \sigma_h$. Under the condition of type III in situ stress, the vertical tensile crack is produced, and the direction of propagation is consistent with the direction of maximum horizontal principal stress. This kind of fracture has weak longitudinal propagation ability. Mudstone about 2 m thick can limit the fracture, but it has strong transverse propagation ability, which can extend nearly one hundred meters. The stress state of type I also produces vertical tensile fracture, and the extension direction is consistent with the direction of the maximum horizontal principal stress. However, different from the stress of type III, the transverse extension ability of the fracture is weak, the longitudinal extension ability is strong, which can cause the phenomenon of layer penetration. The present ground stress type in northeast Sichuan is also type III, and the compressive fracture has strong transverse extension ability, but weak vertical extension ability.

6 Conclusions

In this paper, combined with acoustic emission experimental data and imaging logging data, the characteristics of in situ stress in Northeast Sichuan are studied, and the following conclusions are obtained:

(1) The three principal stress relationships in the northeastern of Sichuan are mainly manifested as $\sigma_H > \sigma_V > \sigma_h$, which are thrust-type stress states, indicating that the horizontal tectonic stress in the studied area is dominant;

(2) The three principal stresses in the northeastern Sichuan basin all increase linearly with the increase of buried depth. Due to the complex tectonic movement of deep marine carbonate strata, the horizontal shear stress and dispersion degree of the strata are greater than that of terrigenous clastic strata;

(3) The horizontal principal stress direction of terrigenous clastic rock formation and Marine carbonate rock formation in eastern Sichuan was determined based on the imaging logging data and dual-hole diameter logging curve, combined with drilling-induced fracture method and borehole caving method. The maximum horizontal principal stress direction in the marine carbonate formation is NE-SW85°. The direction of the maximum horizontal principal stress in the terrane clastic rock formation is basically NW–SE direction, i.e., 97.5°–112.5°.

(4) The fracture direction of marine carbonate strata in northeast Sichuan basin is in good consistency with the horizontal principal stress direction. The in situ stress direction is favorable to the secondary reconstruction of natural fractures.

Authors' contributions XF proposed the idea, analyzed the data and completed this paper. Other authors discussed the structure of this paper.

Declarations

Conflict of interest The authors declare that they have no competing interests.

References

1. Yan CH, Chen Q, Zhou W (2002) Characteristics of the current in-situ stress field of the Penglai Zhen Formation in Luodai Gas Field. Nat Gas Ind 22(2):106–107

2. Zhan FL (2006) The influence of ground temperature gradient on the calculation of ground stress in underground mines. Min Res Dev 6(2):24–36

3. Jing F, Bian ZH, Chen H (2008) Statistical analysis on the distribution of lateral pressure coefficients of different lithologies. J Yangtze River Sci Res Inst 25(4):48–59

4. Li H, Fan CH, Qin QR (2018) Fracture characteristics and its genesis of tight reservoir in Xujiahe formation of central Yuanba area in Sichuan basin. Reserv Eval Dev 8(2):1–6

5. Wang ZH, Hao CG, Li JM (2019) Distribution and genetic mechanism of overpressure in western Sichuan foreland basin. Lithologic Reserv 31(6):36–45

6. Xu ZX, Meng W, Guo WB (2021) In-situ stress measurement and its application of a deep-buried tunnel in Zheduo Mountain. West Sichuan Geosci 35(1):114–126

7. Lin Liangbiao YuY, Guo J (2018) The origin and geochemical characteristics of Permian chert in the Eastern Sichuan Basin. China Carbonates Evaporates 33:613–624

8. Ge HK, Lin YS, Wang SC (1998) In situ stresses determination technique and its applications in petroleum exploration and development. J Univ Pet, China 22(1):94–98

9. Shu Y, Hu M (2010) Structural feature and deformation stages in northeast of Sichuan Basin. Complex Hydrocarbon Reserv 3(2):17–22

10. Xiong ZF, Deng JH, Chen D (2015) The comprehensive evaluation of the deviation factor calculation of natural gas in Northeast Sichuan. J Southeast Pet Univ 37(4):60–68

11. Brady BHG (1985) Rock Mechanics for underground mining. George Allen & Unwin, London

12. Brown ET, Hoek E (1978) Technical note trends in relationships between measured in-situ stress and depth. Int J Rock Mech Min Sci 15:211–215

13. Hudson JA, Harrison JP (1997) Engineering rock mechanics: an introduction to the Principals. Elsevier, Oxford

14. Fuchs K, Muller B (2001) World stress map of the earth: a key to tectonic processes and technological applications 88:357–371

15. Jing F, Sheng Q, Zhang YH (2007) Study on the distribution of measured in-situ stress in the shallow crust of the Chinese mainland. Chin J Rock Soil Mech Eng 26(10):2056–2068

16. Kang HP, Lin J, Zhang X (2010) Study on measurement and distribution of underground stress in Lu'an mining area. Rock Soil Mech 31(3):827–839

17. Zhao DA, Chen ZM, Cai XL (2007) Statistical analysis on the distribution law of in-situ stress field in China. Chin J Rock Mech Eng 26(6):1265–1278

18. Zhu HC, Tao ZY (1994) Preliminary analysis of topography and in-situ stress distribution. Water Resour Hydropower Technol 1(12):27–28

19. Kang HP, Yi BD, Gao FQ (2019) In-situ stress database and in-situ stress distribution law of coal mines in China. J China Coal Soc 44(1):24–36

20. Tang Y, Mei LF, Xiao AC (2013) Transition of tectonic stress field and hydrocarbon significance of the Late Mesozoic-Cenozoic in Xuanhan-Daxian region, northeastern Sichuan Basin. Acta Petrolei Sinica 34(1):59–71

21. Li HJ, Zhou XG, Zhang LY (2009) Carbonate reservoir comparison between Tahe oilfield and Puguang gas field. J Geomech 15(4):396–405

22. Ni XF, Chen HD, Tian JC (2007) Sedimentary framework of Changxing-Feixianguan formations and its control on reservoir in northeastern Sichuan. Oil Gas Geol 28(4):458–465

23. Jiang YL, Li MY, Wang LJ (2020) Characteristics and controlling factors of tight sandstone reservoir fractures of the Xujiahe Formation in the Bazhong-Tongnanba. Northeast Sichuan Acta Geologica Sinica 94(5):1525–1537

24. Bai B, Zou CN, Zhu RK (2012) Development period of structural fractures and its characters in the low permeability sandstone reservoir of the second Member of the Upper Triassic Xujiahe Formation in south of western Sichuan Basin. Acta Geol Sin 86(11):1841–1846

25. Cao HY, Wang W, Liu M (2018) Characteristics of fractures in Xujiahe Formation of Tongnanba structural belt, northeastern Sichuan Basin. Xinjiang Pet Geol 4:424–429

26. Guo M, Li ZD, Yang L (2010) Evolution of abnormal pressure and hydrocarbon accumulation in Feixianguan Formation in the northeastern Sichuan Basin. J Southwest Pet Univ 32(1):175–182

27. Liu Z, Zhu WQ, Sun Q (2012) Characteristics of geotemperature-geopressure system in petroliferous basin of China. Acta Petrolei Sinica 33(1):1–17

28. Su J, Zhang SC (2010) Control of fault system to formation of effective carbonate reservoirs and the rules of petroleum accumulation. Acta Petrolei Sinica 31(2):196–203

29. Su N, Yang W, Yuan BG (2021) Structural features and deformation mechanism of transtensional faults in Himalayan Period. Sichuan Basin Earth Sci 46(7):2362–2380

30. Xu HL, Wei GQ (2012) Tectonic evolution of the Leshan-Longnüsi Paleo-uplift and its control on gas accumulation in the Sinian Strata. Sichuan Basin Pet Explor Dev 39(4):406–416

31. Huang ZQ (2003) Calculate earth stress by acoustic data. Spec Oil Gas Reserv 10(4):4–10

32. Zhao YQ (2009) A Method of analyzing crustal stress orientation using imaging logging. Pet Drill Tech 37(6):39–44

33. Liu JW (2004) The application of multipole array acoustic method on hard formation of Liaohe Oil Field. Geoscience 18(3):378–384

34. Wang P (1992) A geomechanically technique-types and distribution of geostress under various tectonic forces. Acta Petrolei Sinica 13(1):1–12